Draft version October 19, 2016
Preprint typeset using LaTeX style AASTeX6
With modifications by David W. Hogg and Daniel Foreman-Mackey

ROTATING STARS FROM *Kepler* OBSERVED WITH GAIA DR1

James R. A. Davenport[1,2]

[1]Department of Physics & Astronomy, Western Washington University, 516 High St., Bellingham, WA 98225, USA

[2]NSF Astronomy and Astrophysics Postdoctoral Fellow

ABSTRACT

Astrometric data from the recent Gaia Data Release 1 has been matched against the sample of stars from *Kepler* with known rotation periods. A total of 1,299 bright rotating stars were recovered from the subset of Gaia sources with good astrometric solutions, most with temperatures hotter than 5000 K. From these sources, 894 were selected as lying near the main sequence using their absolute G-band magnitudes. These main sequence stars show a bimodality in their rotation period distribution, centered roughly around a 600 Myr rotation-isochrone. This feature matches the bimodal period distribution from cooler stars with *Kepler*, but was previously undetected for solar-type stars due to sample contamination by subgiants. A tenuous connection between the rotation period and total proper motion is found, suggesting the period bimodality is due to the age distribution of stars within ∼300pc of the Sun, rather than a phase of rapid angular momentum loss. This emphasizes the unique power for stellar populations studies of combining temporal monitoring from *Kepler* with astrometric data from Gaia

1. INTRODUCTION

The *Kepler* mission (Borucki et al. 2010) has enabled the first studies of rotation periods for large ensembles of field stars. The fundamental stellar property of rotation has been measured for over 30k stars using the high cadence *Kepler* light curves, tracing the periodic or quasi-periodic modulations in brightness as cool starspots rotate in and out of view (Reinhold et al. 2013; McQuillan et al. 2014). The seminal work by Skumanich (1972) connected stellar rotation and age via angular momentum loss, leading to an age estimating technique known as gyrochronology. At present, ages determined by gyrochronology are accurate to ∼10% in the *best* cases (young solar-type stars). With rotation now being routinely measured, it is hoped a new ability of

determining robust ages for field stars will be possible by calibrating gyro-isochrones to stellar clusters and asteroseismic samples, and improved models of angular momentum loss (e.g. Angus et al. 2015; van Saders et al. 2016).

Curiously, in studying the rotation periods for M dwarfs in the *Kepler* field, McQuillan et al. (2013) discovered a bimodal period distribution, which was subsequently confirmed to exist up to K dwarfs in the *Kepler* field by McQuillan et al. (2014). However, this had never been observed in any other study of stellar rotation periods, including stellar clusters at a variety of ages, nor was it detected in the *Kepler* stars at hotter temperatures ($T_{eff} > 5000$). While binary stars and multiple-period systems may be contaminating the rotation period sample for *Kepler* field stars, McQuillan et al. (2014) found they could not adequately explain the bimodal period distribution. Currently favored explanations for this feature are 1) a non-continuous age distribution for nearby stars, as was suggested with very nearby Hipparcos stars by Hernandez et al. (2000), or 2) a previously unknown phase of rapid angular momentum loss for low-mass stars, similar to the "Vaughan-Preston" gap seen in chromospheric activity indicators (Vaughan & Preston 1980). As independent age indicators for these field stars are often non-existent, and both scenarios deal with physical mechanisms that are not currently understood with precision, a definitive explanation has not been found.

Astrometric data from the Gaia mission (Gaia Collaboration 2016) can help shed light on this stellar population mystery. By measuring distances via stellar parallax for these rotating stars, the *Kepler*–Gaia sample can separate single main sequence dwarfs from binary stars or evolved stars such as subgiants, and will help calibrate fundamental properties of *Kepler* stars, such as log(g) (Creevey et al. 2013). Galactic kinematics from Gaia will also provide an additional age-proxy, and allow for searches of substructure in field star ages such as from moving groups. The Gaia data will also enable a measurement of the star formation history of the disk from both white dwarf cooling sequences (Carrasco et al. 2014; Gaensicke et al. 2015) and color-magnitude diagram models (Bertelli et al. 1999).

In this paper I demonstrate the utility of combining temporal properties derived from *Kepler* light curves with the preliminary astrometric solutions from Gaia Data Release 1 (hereafter DR1 Lindegren et al. 2016). This combined sample allows improved selection of main sequence stars, and reveals previously undetected structure in the rotation period distribution for solar-type stars.

2. THE *Kepler*–GAIA DATA

Rotation periods in this study come from McQuillan et al. (2014), who performed an Auto-Correlation Function analysis of *Kepler* stars cooler than 6500 K that had at least ∼2 years of observation. The periods recovered from this approach generally agree very well with those found via Lomb-Scargle Periodograms (e.g. Reinhold et al. 2013; Aigrain et al. 2015). Sources with multiple distinct periods, such as from binary

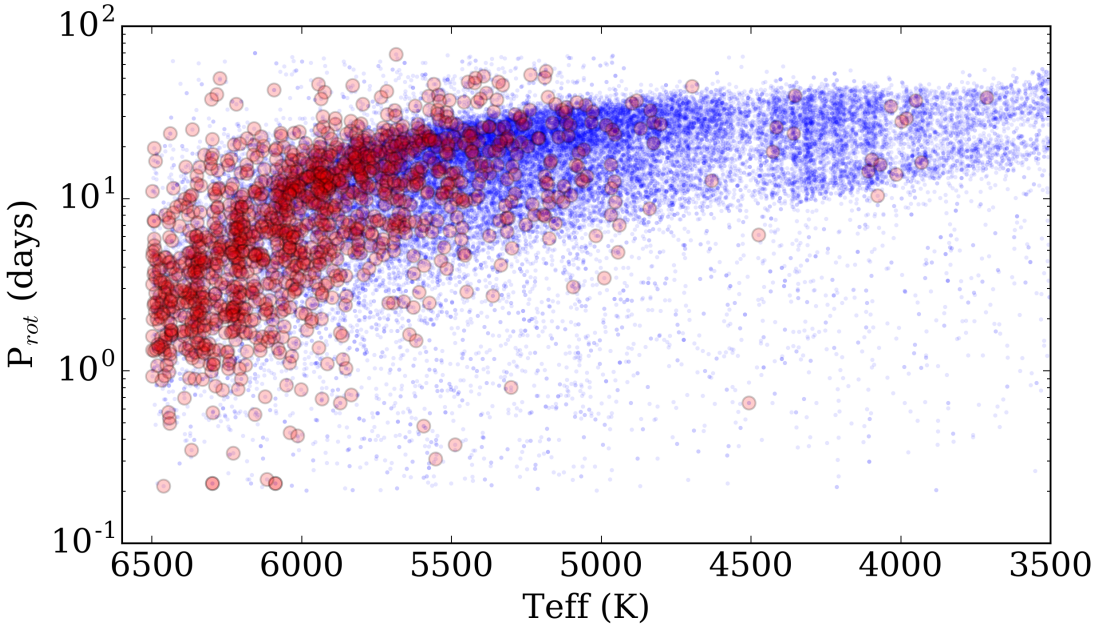

Figure 1. Rotation period distribution for 33,855 *Kepler* stars from McQuillan et al. (2014) with detections in Gaia DR1 (blue dots). The period bimodality can be seen most clearly for stars with $T_{eff} < 4000$ K as a dearth of sources with periods of ∼25 days, but extends to at least $T_{eff} \sim 5500$ K according to McQuillan et al. (2014). The subsample of 1,299 nearby objects found in TGAS are highlighted (red circles), and are mostly hotter stars due to the faint limit of the TGAS sample.

systems with two spotted stars (e.g. Lurie et al. 2015) are detected by McQuillan et al. (2014), but are not included in the following analysis.

The Gaia Data Release 1 (DR1) provides astrometric positions for over 10^9 sources from the first year of observation with Gaia. The Tycho-Gaia Astrometric Solution (TGAS) measures improved proper motions and parallaxes for 2 million nearby, bright sources by extending the astrometric solutions from Tycho and Hipparcos. While the TGAS data are not a complete astrometric survey, and have possible systematics in the reported parallaxes (Stassun & Torres 2016), they represent a significant improvement in the astrometry and kinematics available for stars in the *Kepler* field thanks to the precision of Gaia.

Using the CDS X-Match service, I cross-matched the available catalogs from these two surveys. A default cross-match radius of 5 arcsec was used. A total of 33,855 stars were found in cross match between these catalogs, 99.5% of the sample from McQuillan et al. (2014). A subset of 1,299 objects were recovered in the TGAS sample. Due to the brightness limits of the TGAS sample very few K and M dwarfs were recovered in the TGAS sample. Future releases of Gaia data will ostensibly provide full astrometric solutions for nearly all *Kepler* stars. The rotation periods versus stellar effective temperatures for the *Kepler*–Gaia matched stars are shown in Figure 1.

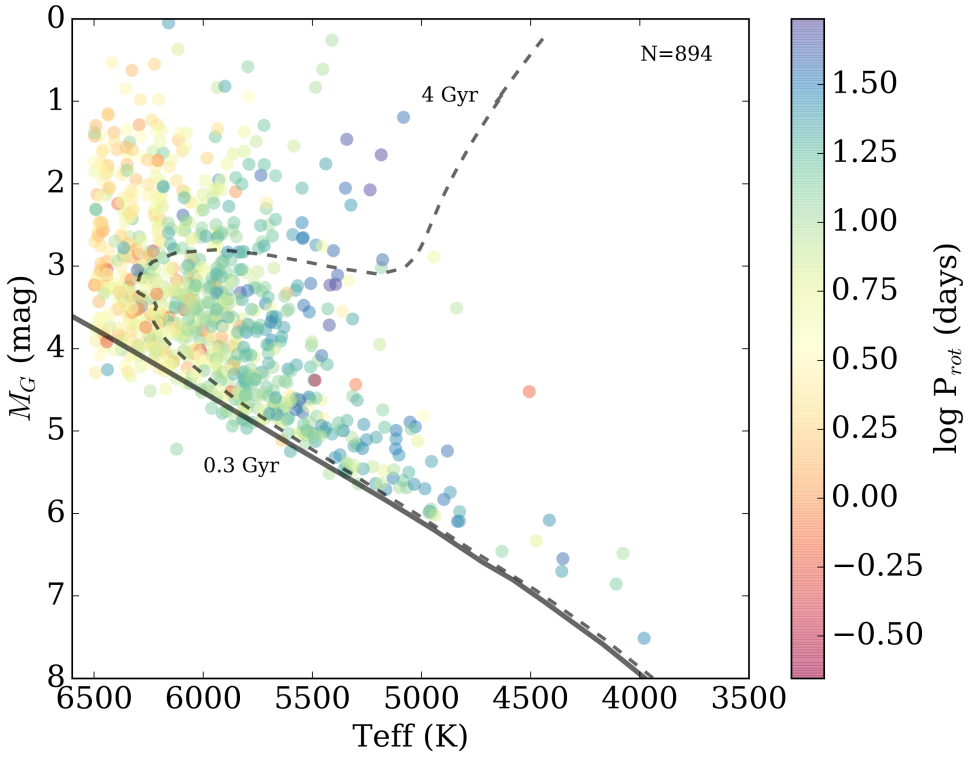

Figure 2. Hertzsprung–Russell (HR) diagram using temperatures from McQuillan et al. (2014) and Gaia DR1 G-band absolute magnitudes for the 894 stars that pass photometric and parallax quality cuts described in the text. Points are colored by their measured *Kepler* rotation periods. Two isochrones from Bressan et al. (2012) are shown, with ages of 300 Myr and 4 Gyr (solid and dashed lines).

3. SELECTING MAIN SEQUENCE STARS

Though McQuillan et al. (2014) attempted to only measure periods for dwarf stars, the sample of *Kepler*–Gaia matched stars contains both main sequence dwarfs and evolved stars (giants and subgiants). Previous studies have shown significant contamination by giants or subgiants can affect the implied variability properties of dwarf stars (Ciardi et al. 2011; Mann et al. 2012). Therefore to properly understand the nature of the period distribution and its implications for age-dating field stars, a robust sample of main sequence stars must be selected.

Faint stars were removed by requiring sources have G-band flux errors $< 1\%$. To ensure accurate distances, and therefore luminosities, parallaxes were required to have errors < 0.4 mas year^{-1}. These cuts left a total of 894 stars from the *Kepler*–TGAS matched sample (68%). The Hertzsprung–Russell (HR) diagram for these stars is shown in Figure 2, with each point colored by its *Kepler*-measured rotation period. Example isochrones from the Bressan et al. (2012) grid are shown for two ages. A systematic offset between the measured absolute G-band and the isochrone main sequence of $\sim$0.5 magnitudes is found (Figure 3).

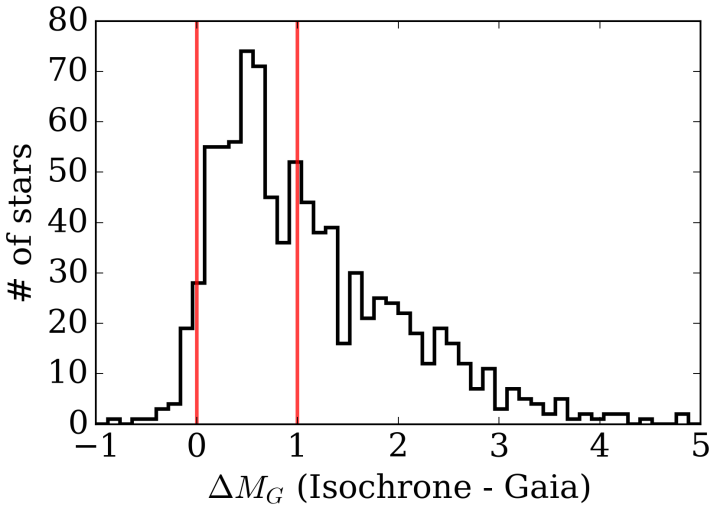

Figure 3. Distribution of differences between the Gaia DR1 G absolute magnitudes and values for main sequence stars from the 300 Myr isochrone shown in Figure 2. The range of sources selected near the single star main sequence (red lines) may have additional contamination due to dust extinction and binary companions.

The HR-period diagram in Figure 2 shows stars with a range of evolutionary states, and could help test post-main sequence angular momentum evolution models (e.g. do Nascimento et al. 2012). Outliers in this diagram (e.g. the rapidly rotating star at T_{eff} = 4500 K, M_G = 4.5 mag, P_{rot}=0.652 d, KIC 07957709) are either due to erroneous cross-matching between the *Kepler* and Gaia catalogs, or represent interesting systems such as rare binary star configurations or stars that have undergone mergers or ingested giant planets (Massarotti 2008; Tayar et al. 2015). Explaining such outliers is beyond the scope of this work, but these targets are worth further study as they may reveal new physics.

The difference between the 300 Myr isochrone main sequence track and the observed M_G is shown in Figure 3. Given the systematic offset of ∼0.5 mag, a fairly wide band of stars ($0 \leq \Delta M_G \leq 1$) was selected as being "close to the main sequence". The final sample included 440 stars. This simplistic cut is not a robust dwarf–giant, nor single–binary star separator, but serves to select a sample of mostly main sequence stars for the illustrative purpose of this work. More precise selection will require an improved isochrone track, as well as updated parallaxes from the full Gaia DR2.

4. EXTENDING THE SPIN-DOWN GAP

A bimodal period distribution was first discovered by McQuillan et al. (2013) for *Kepler* M dwarfs, who found a dearth of objects with periods around ∼25 days. Follow-up work by McQuillan et al. (2014) found this bimodality extended to K dwarfs, up to $T_{eff} \sim 5500$. Figure 4 shows the rotation period distribution for the

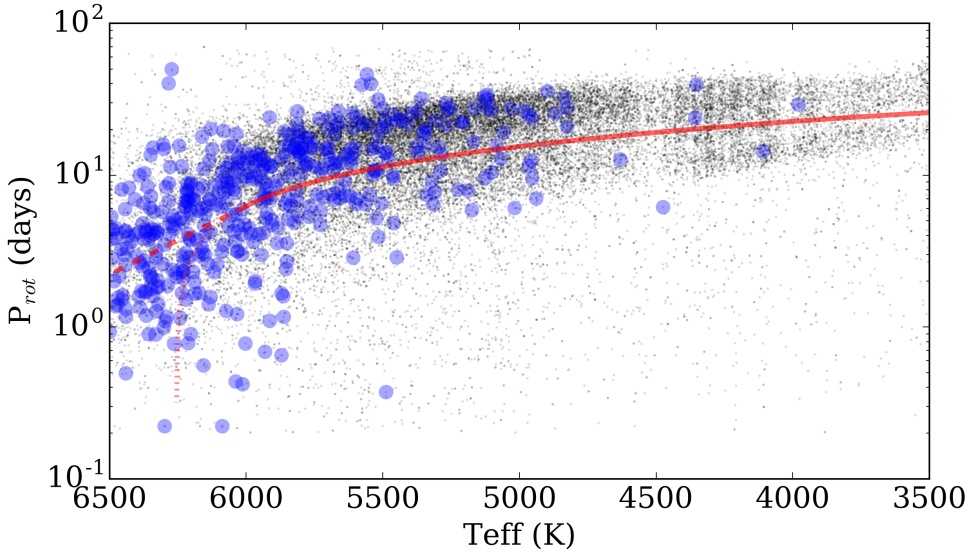

Figure 4. Rotation period versus temperature for TGAS-matched stars near the isochrone main sequence (blue circles). The full *Kepler*–Gaia matched sample is shown for reference (small black dots). A bimodality in rotation periods initially discovered for M dwarfs by McQuillan et al. (2013), extends the full range of temperatures in the *Kepler*–Gaia main sequence sample shown here. A Meibom et al. (2011) 600 Myr gyrochonology-isochrone (gyrochrone) traces the bimodality midpoint up to 6000 K (red solid line), but deviates from the isochrone sharply to ∼6200 K (red dotted line). A log-linear extrapolation of the isochrone at 6000K to 6500 K (red dashed line) continues to track the bimodality to hotter temperatures, and roughly follows a line of constant Rossby number.

final 440 star sample of likely main sequence stars. The bimodality appears to extend smoothly through to the hottest stars in this sample.

While these periods for field stars were robustly measured by McQuillan et al. (2014) and others, the bimodality did not appear in previous *Kepler* work due to the high contamination rate by subgiants for these bluer, hotter stars. 414 rotating stars had acceptable photometric and parallax uncertainties in TGAS, but were culled from this sample for having M_G luminosities higher than the main sequence cut in §3 above. Note that distributions of $\log g$ values from the Kepler Input Catalog (Brown et al. 2011) for both the main sequence and subgiant stars were not statistically different.

The minimum in the bimodal period distribution in Figure 4 can be traced using a gyrochonology isochrone (colloquially known as a "gyrochrone"). Many different studies have produced competing gyrochrone models, each with unique morphologies at the hot and cool star regimes (e.g. Barnes 2007; Mamajek & Hillenbrand 2008; Meibom et al. 2011; Angus et al. 2015). A 600 Myr gyrochrone from Meibom et al. (2011) was determined by eye to approximately trace the period minima from 3500 K to 6000 K. As shown in Figure 4, this model (as with most gyrochronology models) turns down in period sharply for stars hotter than ∼6000 K. A log-linear extrapolation of the 600 Myr gyrochrone at 6000 K continues to trace the period bimodality up to 6500 K, and roughly traces a line of constant Rossby number.

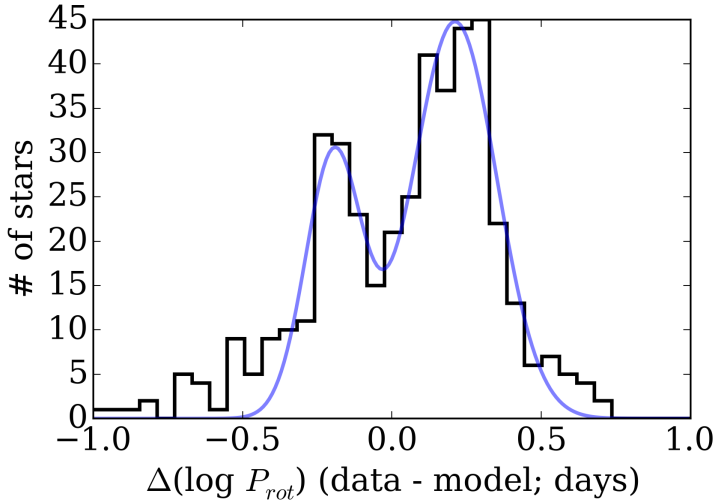

Figure 5. Residual of log rotation periods about the Meibom et al. (2011) 600 Myr gyrochrone, using the log-linear extrapolation between 6000–6500 K shown in Figure 4. The bimodal rotation period distribution is clear, with peaks at $\Delta \log P_{rot}$ of -0.19 and 0.21 days. A two-Gaussian model was fit to this distribution (blue line). Approximately 50% more stars are present in the slower, nominally older peak (right).

The difference (in log period) between the observed rotation and the 600 Myr gyrochrone for the 440 likely main sequence stars is shown in Figure 5. Despite combining stars of all temperatures, the bimodality is clearly seen in this log period space. A two Gaussian model was fit to this data, which found peaks in the two periods distributions of -0.19 ± 0.01 and 0.21 ± 0.01 days. 262 stars had periods longer than the gyrochrone model (right peak) and 178 slower than the model (left peak). This is in contrast to the overall results from McQuillan et al. (2013) who found nearly equal numbers of M dwarfs in the fast and slow rotating groups, but is in general agreement with their sample with non-zero proper motions.

this age explanation was bolstered in McQuillan et al. (2013), who noted the two populations of rotating M dwarfs had different distributions of proper motions, indicating they belonged to distinct groups of stars. The distribution of total proper motion for stars above and below the modified 600 Myr gyrochrone is shown in Figure 6. Stars above the gyrochrone (slower rotators, nominally older) have a median total proper motion of 15.4 mas/yr, while those below (faster rotators, younger) have a median of 11.3 mas/yr. This difference in kinematics versus rotation period is in the same direction observed by McQuillan et al. (2013). As the typical error in the total proper motion is ∼1.4 mas/yr for this sample, this is a marginal (2.8σ) difference. Note also that likely contamination of subgiants in the hotter stars may also obscure kinematic differences.

5. DISCUSSION

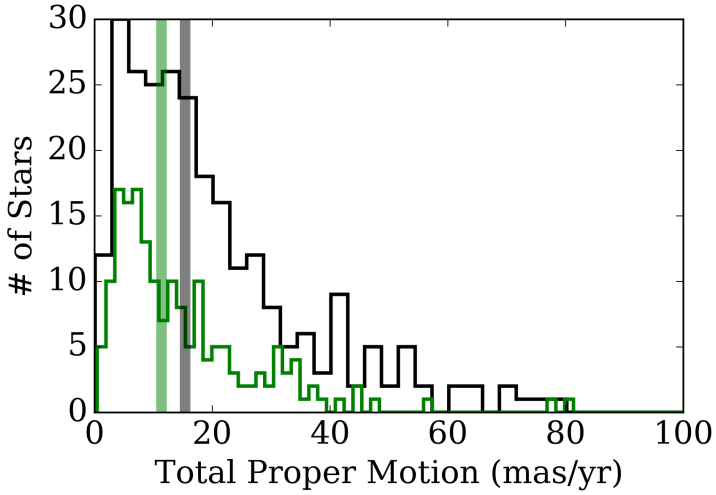

Figure 6. Total proper motion distributions for stars above (rotating slower, older stars) the gyrochrone model shown in Figure 4 (black) and below (rotating faster, younger stars) the model (green). Median values of the two distributions are shown (thick lines), which yield a marginal 2.8σ difference.

median distance of K/M stars ($T_{eff} > 4000$ K) is ∼216 pc, using isochrone median distance for the TGAS-matched sample (blue points) is very close, 285 pc, so also sampling just the most local volume. this points to the effect being localized around us, which explains why it has not been seen in other gyro studies to date (e.g. clusters) Unfortunately not enough rotation period data across the fully convective boundary (∼3000 K) to tell if this bimodal feature continues.

the bimodality may be another manifestation of the "Vaughan Preston gap" (Vaughan & Preston 1980), e.g. discussed for rotating stars byKado-Fong et al. (2016). either due to fast evolution through intermediate stellar activity, or could be an age gap. if age, these clumps line up roughly with a 300 Myr and 2 Gyr Meibom et al. (2011) gyro-isochrone from cooler than about 6000 K. this similar to the non-continusous star formation history for the local solar neighborhood using Hipparcos astrometry (Hernandez et al. 2000).

finally, have shown utility for using Gaia data, combined with detailed light curve statitiscs from *Kepler*, to reveal hidden structure in properties of field stars. This combination will be super useful for determining approximate log g values (separating main sequence from sub-giants), and thus more accurate gyrochronology ages (van Saders & Pinsonneault 2013). also for modeling the star formation history of the entire milky way (e.g. Bertelli et al. 1999).

Special thanks to Jennifer van Saders, Sean Matt, and Travis Metcalfe for their helpful discussions that motivated publishing this work.

JRAD is supported by an NSF Astronomy and Astrophysics Postdoctoral Fellowship under award AST-1501418.

This research made use of the cross-match service provided by CDS, Strasbourg.

REFERENCES

Aigrain, S., Llama, J., Ceillier, T., et al. 2015, MNRAS, 450, 3211
Angus, R., Aigrain, S., Foreman-Mackey, D., & McQuillan, A. 2015, MNRAS, 450, 1787
Barnes, S. A. 2007, ApJ, 669, 1167
Bertelli, G., Bressan, A., Chiosi, C., & Vallenari, A. 1999, Baltic Astronomy, 8, 271
Borucki, W. J., Koch, D., Basri, G., et al. 2010, Science, 327, 977
Bressan, A., Marigo, P., Girardi, L., et al. 2012, MNRAS, 427, 127
Brown, T. M., Latham, D. W., Everett, M. E., & Esquerdo, G. A. 2011, AJ, 142, 112
Carrasco, J. M., Catalán, S., Jordi, C., et al. 2014, A&A, 565, A11
Ciardi, D. R., von Braun, K., Bryden, G., et al. 2011, AJ, 141, 108
Creevey, O. L., Thévenin, F., Basu, S., et al. 2013, MNRAS, 431, 2419
do Nascimento, J.-D., da Costa, J. S., & Castro, M. 2012, A&A, 548, L1
Gaensicke, B., Tremblay, P.-E., Barstow, M., et al. 2015, ArXiv e-prints, arXiv:1506.02653
Gaia Collaboration. 2016, ArXiv e-prints, arXiv:1609.04153
Hernandez, X., Valls-Gabaud, D., & Gilmore, G. 2000, MNRAS, 316, 605
Kado-Fong, E., Williams, P. K. G., Mann, A. W., et al. 2016, ArXiv e-prints, arXiv:1608.00978
Lindegren, L., Lammers, U., Bastian, U., et al. 2016, ArXiv e-prints, arXiv:1609.04303
Lurie, J. C., Davenport, J. R. A., Hawley, S. L., et al. 2015, ApJ, 800, 95
Mamajek, E. E., & Hillenbrand, L. A. 2008, ApJ, 687, 1264
Mann, A. W., Gaidos, E., Lépine, S., & Hilton, E. J. 2012, ApJ, 753, 90
Massarotti, A. 2008, AJ, 135, 2287
McQuillan, A., Aigrain, S., & Mazeh, T. 2013, MNRAS, 432, 1203
McQuillan, A., Mazeh, T., & Aigrain, S. 2014, ApJS, 211, 24
Meibom, S., Barnes, S. A., Latham, D. W., et al. 2011, ApJL, 733, L9
Reinhold, T., Reiners, A., & Basri, G. 2013, A&A, 560, A4
Skumanich, A. 1972, ApJ, 171, 565
Stassun, K. G., & Torres, G. 2016, ArXiv e-prints, arXiv:1609.05390
Tayar, J., Ceillier, T., García-Hernández, D. A., et al. 2015, ApJ, 807, 82
van Saders, J. L., Ceillier, T., Metcalfe, T. S., et al. 2016, Nature, 529, 181
van Saders, J. L., & Pinsonneault, M. H. 2013, ApJ, 776, 67
Vaughan, A. H., & Preston, G. W. 1980, PASP, 92, 385